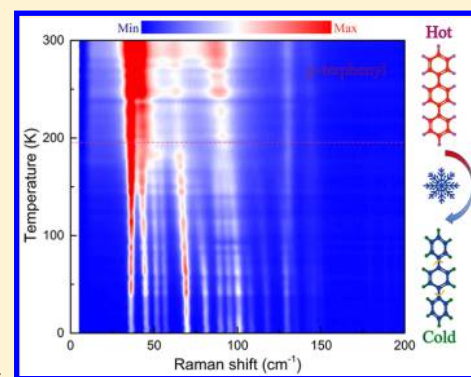


Vibrational Properties of *p*-TerphenylKai Zhang,^{†,‡,§} Ren-Shu Wang,[§] and Xiao-Jia Chen^{*,§}HPSTAR
617-2018[†]Key Laboratory of Materials Physics, Institute of Solid State Physics, Chinese Academy of Sciences, Hefei 230031, China[‡]University of Science and Technology of China, Hefei 230026, China[§]Center for High Pressure Science and Technology Advanced Research, Shanghai 201203, China

ABSTRACT: Vibrational properties associated with the intra- and intermolecular terms of pristine *p*-terphenyl at low temperatures are analyzed in detail by Raman spectroscopy. Nearly all of the vibrational modes exhibit anomalous behaviors at the transition temperature of about 193 K on the frequencies, widths, and intensities. Meanwhile, the drastic drops of the spectrum weight result in the splits of many peaks like the lattice vibrational peaks and the peaks located at around 1220, 1280, and 1600 cm⁻¹. All the anomalies result from the drastic decrease of the vibrational anharmonic coupling effects in the crystalline *p*-terphenyl after entering into the ordered state. The rapidly declining anharmonicity also makes contributions to the anomalous behaviors of the intensity ratios of the 1220, 1280, and 1600 cm⁻¹ modes, as well as the energy separations between the combination bands and the fundamental bands. Our work is of great significance to understand the internal vibrational properties of *p*-terphenyl.



■ INTRODUCTION

Poly(*para*-phenylene) (PPP) materials, as the excellent chemical and thermal properties, have received a lot of attention in the scientific research and application areas. The pristine PPP materials always exhibit insulating or semi-conducting state. However, previous works discovered that the conductivity of these materials can have drastic increases of magnitude after electrons donors or acceptors doping.^{1–3} Recently, superconductivity is found in the potassium-doped PPP materials.^{4–9} These findings open an encouraging window for the exploration of high temperature even room temperature superconducting transition in organic materials. The drastic increase on the conductivity in PPP materials also makes these materials good potential in the thermoelectric applications.^{10–12} PPP materials all have the structure with phenyl rings connecting at the *para* positions. Such a typical structure results in two major forces with contrary effects.^{13,14} One is the steric repulsion, this force tends to distort the neighboring phenyl rings perpendicular to each other. The other force arises from the delocalized π -electrons and mostly contributes to make the phenyl rings in one molecule parallel. These two competitive forces, as a result, lead to strong thermal librations on the molecules around the long molecular axes. However, previous works based on X-ray and neutron diffraction experiments discovered that the individual molecules of PPP materials show planar states on average at ambient condition.^{15–18} At low temperatures, the interring tilt angle of the molecules reemerges as the freeze of the molecular librations; i.e., the molecules become nonplanar.^{15–18} Interestingly, the adjacent molecules are confirmed to have opposite torsion angles along the *a* and *b* crystal axes. Hence, the lattice parameters *a* and *b* have double enlargements. Such structural

phase transitions among PPPs are generally classified into “displacive” and “order–disorder” types. Biphenyl was found to be the only “displacive” type transition, and the *p*-terphenyl structural phase transition was predicted near the boundary between the “order–disorder” and “displacive” regimes.^{16,19} Plenty of works have been performed on the “displacive” type transition in biphenyl,^{20–24} but only a few works focused on the “order–disorder” type. Since the finding of superconductivity with the 123 K transition temperature in potassium-doped *p*-terphenyl,^{6,25} the properties of the *p*-terphenyl become increasingly interesting and important.

p-Terphenyl molecule contains three phenyl rings connected by the single C–C bond. It is often used as ultraviolet laser dye.²⁶ The crystalline *p*-terphenyl has a monoclinic structure with two planar molecules in one unit cell. At around 193 K, it undergoes a order–disorder phase transition.^{21,27–31} The shake angles between the adjacent molecules along the *a* and *b* crystal axes are confirmed in opposite senses. Thus, the lattice parameters have double enlargements on these two directions. The structure transforms to a pseudomonoclinic cell containing eight molecules, or it could adopt a triclinic phase with four inequivalent molecules.^{29,32} The Raman spectroscopy is one powerful tool to detect the phase transitions in PPP materials. The low-frequency Raman study on *p*-terphenyl at low temperature confirmed the order–disorder phase transition.^{20,28,33} In addition, *p*-terphenyl has a more displacive reconstructive transition under pressure,^{34–37} and the influence of the pressure on the structure is also

Received: June 7, 2018

Revised: August 1, 2018

Published: August 1, 2018

studied by Raman scattering.^{34,38} However, to date, few analyses on the *p*-terphenyl intramolecular vibration modes have been performed to study the phase transition. Thus, comprehensive analyses on the internal vibrational properties of *p*-terphenyl, especially the behaviors of the high-frequency range modes, are interesting and essential for the further study.

In this work, we measure the temperature dependent Raman spectra of *p*-terphenyl from 5 to 300 K. The wavelength of the applied beamline is 660 nm. The comprehensive analyses of the vibrational modes from the lattice vibrations to the high-frequency modes of C–H vibrations are introduced to study the order–disorder phase transition occurring at around 193 K. Our work is of important significance to understand the internal properties of *p*-terphenyl, and it provides the basis for the further studies on *p*-terphenyl.

EXPERIMENTAL DETAILS

In this experiment the high-purity sample was purchased from Alfa Aesar. It was sealed in a quartz tube with the diameter of 1 mm for Raman-scattering experiments in a glovebox with the moisture and oxygen levels less than 0.1 ppm. The wavelength of the exciting laser beam was 660 nm. The power was less than 1 mW before a $\times 20$ objective to avoid possible damage of the sample. An integration time of 20 s was used to obtain the spectra. The scattered light was focused on a 1200 g/mm grating and then recorded with a 1024 pixel charge coupled device designed by Princeton. A continuous-flow liquid-helium cryostat was used to obtain a low-temperature condition from 5 to 300 K, and a vacuum pump was used to assist in achieving the temperature less than 40 K.

RESULTS AND DISCUSSION

Figure 1 shows the 660 nm laser excited Raman spectra of *p*-terphenyl at 300, 200, 100, and 5 K. All the spectra are placed on the same standard scale. Classifications of the vibration

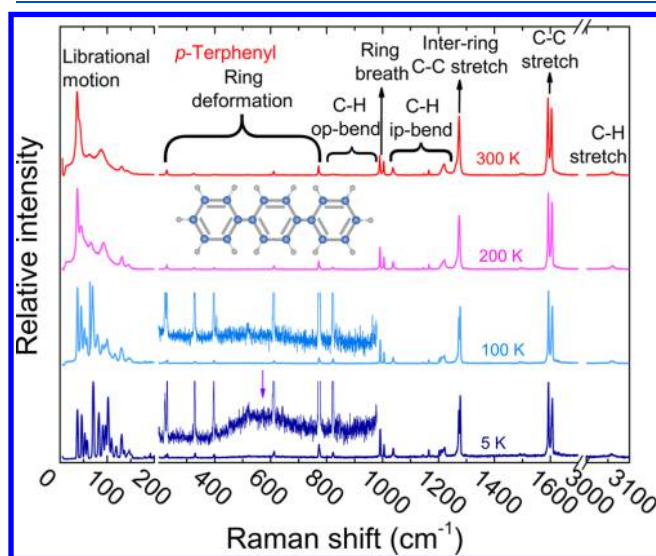


Figure 1. 660 nm laser excited Raman spectra of *p*-terphenyl at 300, 200, 100, and 5 K. The spectra at 5 and 100 K with the frequencies range of 300–980 cm^{-1} have been zoomed in for clarity. A broad hill located at around 500 cm^{-1} with the full width at half-maximum above 100 cm^{-1} is pointed out by a purple arrow. Classifications of the vibration modes over the spectrum of 300 K were taken from ref 37. Here, ip = in-plane and op = out-of-plane.

modes are depicted over the spectrum at 300 K, and the schematic drawing of the *p*-terphenyl molecule is presented over the spectrum at 200 K. All the spectra are broken between 1700 and 3000 cm^{-1} where no phonon bands are observed. At high temperature, the phonon bands in the *p*-terphenyl spectra show very broad features and often overlap to some indistinguishable peaks. However, at low temperature, the spectra show obvious splits on some peaks, especially the librational motion part, the modes at around 1220 and 1280 cm^{-1} , and the highest-frequency C–H stretching modes. Otherwise, unlike the biphenyl, no new peaks except a broad hill located at around 500 cm^{-1} with the full width at half-maximum (fwhm) above 100 cm^{-1} are observed appearing after the structural transition. This indicates that the phase transitions in biphenyl and *p*-terphenyl belong to different types. Two ring breathing modes are observed at around 1000 cm^{-1} . It is different from biphenyl in which one can only observe one ring breathing peak. Such phenomenon most probably results from the different situations existing in the terminal rings and the middle ring of *p*-terphenyl. The energies of these two modes all increase with decreasing temperature, whereas their intensities exhibit different tendencies; the former intensity has almost no changes, and the latter decreases in intensity as the temperature is decreased.

Details of the temperature evolution of the *p*-terphenyl Raman spectra in the lattice vibration range are presented in Figure 2a. All the broad phonon modes observed in this figure have obvious blue shift with decreasing temperature, and they simultaneously decrease their fwhms, together with increased intensities. Below around 200 K, the fwhm of these peaks all have drastic decreases, this results in the splits of those peaks as observed in the figure. At 5 K, the number of the observed

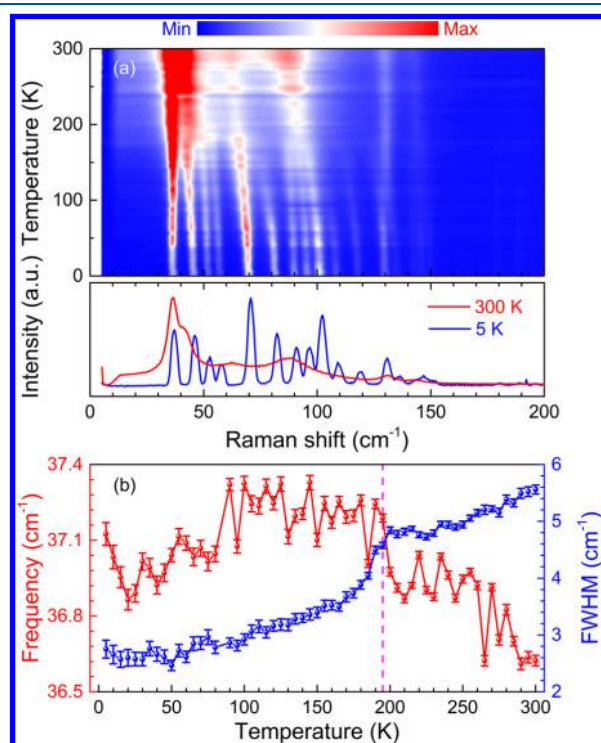


Figure 2. (a) Low-frequency Raman spectra of *p*-terphenyl. (b) Temperature dependent frequency and fwhm of the lowest-frequency mode. The vertical dashed line indicates the structural transition temperature at around 193 K.

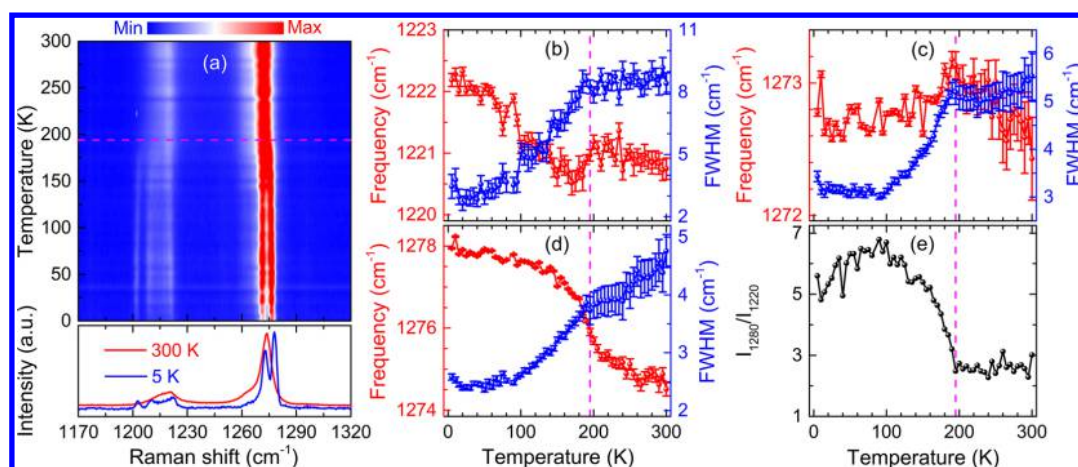


Figure 3. (a) Raman spectra of *p*-terphenyl at the frequencies around 1220 and 1280 cm^{-1} . The inset is the atomic displacement. (b), (c), (d) Frequencies and fwhm of the vibration modes at around 1220 and 1270 cm^{-1} . (e) Intensity ratio of the 1280 cm^{-1} mode and the 1220 cm^{-1} mode. The vertical dashed lines indicate the structural transition temperature at around 193 K.

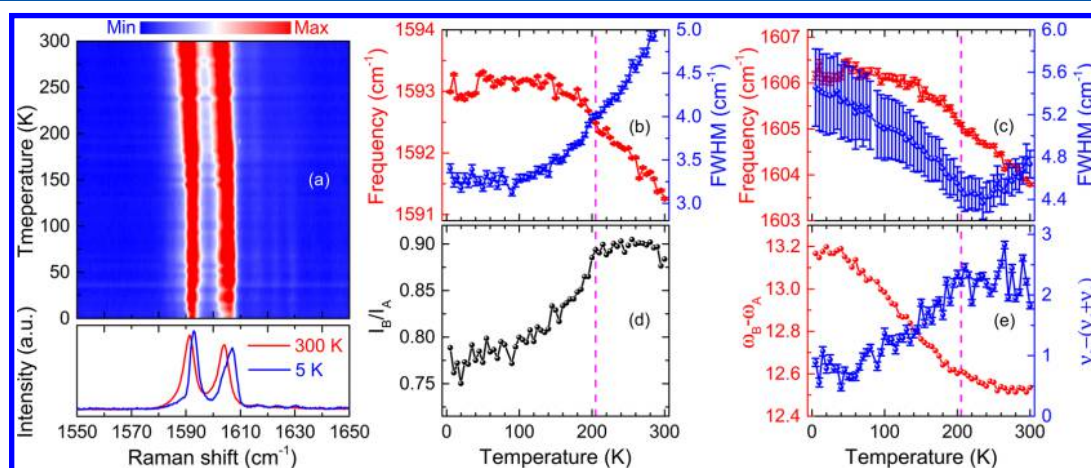


Figure 4. (a) Raman spectra of *p*-terphenyl at the frequency of around 1600 cm^{-1} . The inset is the atomic displacement pattern of the C–C stretching mode. (b), (c) Temperature dependent frequencies and the fwhm of the two peaks at around 1600 cm^{-1} . (d) Temperature dependent intensity ratio I_B/I_A . (e) Difference between these two peaks (red line) and the difference of the $\nu_6 + \nu_1$ and ν_8 (blue line) as a function of temperature. The vertical dashed lines indicate the structural transition temperature.

peaks is 20, this result is consistent with the previous works.^{20,33} We fit the lowest-energy peak by the Lorentz function. This peak is assumed to be associated with the *c* axis, and it is always used as an indicator of the chain lengths of the individual PPP molecules.^{39,40} The fitted results are shown in Figure 2b. The frequency increases with decreasing temperature. At around 193 K, it stops increasing, and then almost stabilizes to constant upon cooling. The temperature dependent fwhm of this mode exhibits the opposite tendency. It has a slight decrease upon cooling. Below 193 K, the fwhm shows a sudden drop. Such a phenomenon indicates that the anharmonic effect is significantly suppressed below 193 K. It also implies that the lattice enters into an ordered state from a chaotic state. This scenario is well in accord with the order–disorder transition case. The other lattice vibration modes also have similar behaviors. This is why those modes exhibit sudden splits shown in Figure 2a after entering into the order state.

Figure 3a presents the temperature evolutionary Raman spectra in the range from 1170 to 1320 cm^{-1} . Two strong peaks located at around 1220 and 1280 cm^{-1} and a weak shoulder near the 1280 cm^{-1} mode can be observed at room temperature. At low temperatures, these peaks all have severe

splits, especially the 1220 cm^{-1} mode, which splits at least four peaks below 200 K. In order to analyze the behaviors of these modes, we respectively fit the two peaks with the strongest intensities at around 1220 and 1280 cm^{-1} by a Lorentzian function. Results are shown in Figure 3b–d. The 1220 cm^{-1} mode exhibits a monotonous increase on the energy with decreasing temperature, but the fwhm of this mode has a sharp drop at around 193 K. The frequencies of the splitting two peaks at around 1280 cm^{-1} exhibit different tendencies, the lower energy peak almost has a stable energy, whereas the frequency of the higher energy peak rapidly increases at around 193 K. The fwhms of these two peaks all exhibit sharp drops at 193 K. The tendencies of these peaks not only are the reasons for peak splits but also indicate the reduction of the anharmonic effect. This is caused by the occurrence of the “order–disorder” type transition. Meanwhile, the intensity of the 1220 cm^{-1} mode reduces obviously below 193 K, whereas the 1280 cm^{-1} mode exhibits little response with the temperature except those modes in the Raman spectra below 40 K. These may result from the additional assistance of the vacuum pump to cool down the sample. This scenario is very consistent with the previous calculations,⁴¹ which reported that

the 1220 cm^{-1} mode is more sensitive to the conjugation than the 1280 cm^{-1} mode. The intensity ratio of these two modes is always used to be an indicator of the chain length and the planarity of the PPP molecules.^{40–44} Figure 3e presents their intensity ratio as a function of temperature. This ratio is almost constant above the transition temperature, whereas it shows a drastic increase below 193 K.

Modes at around 1600 cm^{-1} also attract intense interest due to their interesting vibrational behaviors. These two modes are associated with the C–C stretching E_{2g} modes ν_8 , and they are believed to result from the “resonance splitting”.^{40,45–48} The lower energy peak (A) is the fundamental band, and the higher energy peak (B) is a combination tone from the E_{2g} fundamental ν_1 at around 992 cm^{-1} and the E_{2g} fundamental ν_6 at around 606 cm^{-1} . Figure 4a presents the Raman spectra of *p*-terphenyl at different temperatures. Unlike those in crystalline biphenyl, no obvious splits can be observed in the Raman spectra at low temperature, but an anomalous asymmetry occurs on the higher energy peak. This anomaly looks like the split of this peak. These two peaks were fitted by a Lorentzian function, and the temperature dependent frequencies and fwhms of these two peaks are shown in Figure 4b,c. Both of these modes increase their energies with decreasing temperature. Below the transition temperature, their frequencies become constant. The fwhm of the lower energy peak decreases with decreasing temperature, whereas the fwhm of the higher energy peak exhibits anomalous behavior. It has a downward shift as the temperature is decreased, and then it starts to increase below around 205 K. The big error bar in Figure 4c is due to the additional peak asymmetry. This indicates that this peak starts to split at around 205 K, which can be observed from the emerging shoulder near the higher energy peak. The strong overlap of these peaks makes it hard to be fitted and analyzed. Interestingly, the temperature of 205 K is a little higher than the transition temperature of 193 K. This may signal the entrance of the thermal anomalous state; it has been discovered by thermodynamic studies that the transition in *p*-terphenyl starts above 193 K.^{21,27} This can also be observed in other vibration modes (see Figures 2 and 3).

Figure 4d is the intensity ratio of these two modes. The intensity ratio of the two modes at around 1600 cm^{-1} is also a common indicator of the molecular length and planarity in PPP materials.^{40,42,45} The ratio is almost constant at the normal state, whereas it rapidly drops below around 205 K. This drop results from the structural transition. The difference between peaks A and B and the energy separation between the combination mode ν_8 and the fundamental bands $\nu_6 + \nu_1$ as a function of temperature are shown in Figure 4e. The former is also often used to estimate the planarization.⁴⁹ It shows a drastic increase at low temperature. The latter is an indicator of the mode mixing level. It exhibits an anomalous drop after entering into the order state. The reduction of the difference indicates that the mixing between the fundamental and combination band declines.

According to previous theoretical works,^{41,45} the planarity plays an important role in the vibrational properties. The *p*-terphenyl molecules exhibit strong thermal librations around the *c* axes in the disorder state, and they suddenly quiet down after the “order–disorder” type transition.^{21,28–31} In our work, the intensity ratio of the 1280 cm^{-1} mode and the 1220 cm^{-1} mode, as well as the intensity ratio of the two modes at around 1600 cm^{-1} , remains constant down to the transition temper-

ature. This indicates that the amplitude of the interring librations does not change until 193 K. Upon cooling, almost all the modes rapidly decrease their fwhms. Thus, the anharmonicity inside the crystalline *p*-terphenyl has a significant decrease. This is also the reason for the appearance of the stable interring tilt angle of the molecule. Meanwhile, the diminishing anharmonicity implies the gradual increase of the molecular planarity even though the stable interring tilt angles appear. As a result, these two intensity ratios will decrease, as well as the energy separation of the 1600 cm^{-1} modes increasing and the Fermi resonance decreasing.^{41,45} The vibrational behaviors of the modes at around 1600 cm^{-1} are in accord with this scenario, whereas the intensity ratio of the 1280 cm^{-1} mode and the 1220 cm^{-1} mode is contrary to it. This anomaly should result from the interring tilt angles. In such a way, the two major forces have contrary effects below the transition temperature. As the angles increase, the vibrational amplitude of the interring C–C stretching mode (1280 cm^{-1}) increases and the C–H ip-bending mode (1220 cm^{-1}) decreases. Thus, the intensity ratio of these two modes increases. At low temperatures, the behaviors of the 1600 cm^{-1} modes are better indicators to investigate the vibrational properties.

CONCLUSIONS

In conclusion, we have comprehensively investigated the vibrational properties of the crystalline *p*-terphenyl in the temperature range from 5 to 300 K by the 660 nm laser excited Raman scattering measurement. The librational modes all increase their energies with decreasing temperature, and those peaks exhibit obvious splits that result from the drastic reduction of the width after entering into the “order” state from the “disorder” state at around 193 K. The 1220 and 1280 cm^{-1} modes also have severe splits and the intensity ratio of these two modes shows a rapid increase below the transition temperature. The energies of the 1600 cm^{-1} modes all increase with decreasing temperature. The ratio of the intensity and the difference of these two modes, as well as the difference between ν_8 and $\nu_6 + \nu_1$, all exhibit anomalies at around the transition temperature. All those anomalies are considered to be the signature of the drastic decrease of the anharmonicity inside the crystalline *p*-terphenyl after entering into the order state. Our work is of important significance to understand the internal properties of the *p*-terphenyl, and it provides the basis for the further studies on *p*-terphenyl, especially the exploration the superconducting mechanism in the potassium-doped *p*-terphenyl.

AUTHOR INFORMATION

Corresponding Author

*X.-J. Chen. E-mail: xjchen@hpstar.ac.cn.

ORCID

Kai Zhang: 0000-0001-9959-319X

Notes

The authors declare no competing financial interest.

ACKNOWLEDGMENTS

This work was supported by the National Key R&D Program of China (Grant No. 2018YFA0305900).

REFERENCES

- (1) Havinga, E. E.; Van Horsen, L. W. Dependence of the Electrical Conductivity of Heavily-Doped Poly-*p*-Phenylenes on the Chain Length. *Synth. Met.* **1986**, *16*, 55–70.
- (2) Ivory, D. M.; Miller, G. G.; Sowa, J. M.; Shacklette, L. W.; Chance, R. R.; Baughman, R. H. Highly Conducting Charge-Transfer Complexes of Poly(*p*-Phenylene). *J. Chem. Phys.* **1979**, *71*, 1506–1507.
- (3) Shacklette, L. W.; Eckhardt, H.; Chance, R. R.; Miller, G. G.; Ivory, D. M.; Baughman, R. H. Solid-State Synthesis of Highly Conducting Polyphenylene From Crystalline Oligomers. *J. Chem. Phys.* **1980**, *73*, 4098–4102.
- (4) Wang, R. S.; Gao, Y.; Huang, Z. B.; Chen, X. J. Superconductivity in *p*-Terphenyl. arXiv:1703.05803; <https://arxiv.org/abs/1703.05803>.
- (5) Wang, R. S.; Gao, Y.; Huang, Z. B.; Chen, X. J. Superconductivity at 43 K in a Single C-C Bond Linked Terphenyl. arXiv:1703.05804; <https://arxiv.org/abs/1703.05804>.
- (6) Wang, R. S.; Gao, Y.; Huang, Z. B.; Chen, X. J. Superconductivity Above 120 K in a Chain Link Molecule. arXiv:1703.06641; <https://arxiv.org/abs/1703.06641>.
- (7) Yan, J. F.; Wang, R. S.; Zhang, K.; Chen, X. J. Observation of Meissner Effect in Potassium-Doped *p*-Quaterphenyl. arXiv:1801.08220; <https://arxiv.org/abs/1801.08220>.
- (8) Huang, G.; Wang, R. S.; Chen, X. J. Observation of Meissner Effect in Potassium-Doped *p*-Quinquephenyl. arXiv:1801.06324; <https://arxiv.org/abs/1801.06324>.
- (9) Zhong, G. H.; Wang, X. H.; Wang, R. S.; Han, J. X.; Zhang, C.; Chen, X. J.; Lin, H. Q. Structural and Bonding Characteristics of Potassium-Doped *p*-Terphenyl Superconductors. *J. Phys. Chem. C* **2018**, *122*, 3801–3808.
- (10) Dubey, N.; Leclerc, M. Conducting Polymers: Efficient Thermoelectric Materials. *J. Polym. Sci., Part B: Polym. Phys.* **2011**, *49*, 467–475.
- (11) Xuan, Y.; Liu, X.; Desbief, S.; Leclère, P.; Fahlman, M.; Lazzaroni, R.; Berggren, M.; Cornil, J.; Emin, D.; Crispin, X. Thermoelectric Properties of Conducting Polymers: The Case of Poly(3-Hexylthiophene). *Phys. Rev. B: Condens. Matter Mater. Phys.* **2010**, *82*, 115454.
- (12) Bubnova, O.; Khan, Z. U.; Malti, A.; Braun, S.; Fahlman, M.; Berggren, M.; Crispin, X. Optimization of the Thermoelectric Figure of Merit in the Conducting Polymer Poly(3,4-Ethylenedioxythiophene). *Nat. Mater.* **2011**, *10*, 429–433.
- (13) Carreira, L. A.; Towns, T. G. Raman Spectra and Barriers to Internal Rotation: Biphenyl and Nitrobenzene. *J. Mol. Struct.* **1977**, *41*, 1–9.
- (14) Soto, J.; Hernández, V.; López Navarrete, J. T. Conformational Study and Lattice Dynamics of Poly(*p*-Phenylene): Oligomers and Polymer. *Synth. Met.* **1992**, *51*, 229–238.
- (15) Charbonneau, G. P.; Delugeard, Y. Biphenyl: Three-Dimensional Data and New Refinement at 293 K. *Acta Crystallogr., Sect. B: Struct. Crystallogr. Cryst. Chem.* **1977**, *33*, 1586–1588.
- (16) Baudour, P. J. L.; Cailleau, H.; Yelon, W. B. Structural Phase Transition in Polyphenyls. IV. Double-Well Potential in the Disordered Phase of *p*-Terphenyl From Neutron (200 K) and X-Ray (Room-Temperature) Diffraction Data. *Acta Crystallogr., Sect. B: Struct. Crystallogr. Cryst. Chem.* **1977**, *33*, 1773–1780.
- (17) Baudour, J. L.; Delugeard, Y.; Rivet, P. Structural Phase Transition in Polyphenyls. IV. Crystal Structure of the Low-Temperature Ordered Phase of *p*-Quaterphenyl at 110 K. *Acta Crystallogr., Sect. B: Struct. Crystallogr. Cryst. Chem.* **1978**, *34*, 625–628.
- (18) Delugeard, Y.; Desuche, J.; Baudour, J. L. Structural Transition in Polyphenyls. II. The Crystal Structure of the High-Temperature Phase of Quaterphenyl. *Acta Crystallogr., Sect. B: Struct. Crystallogr. Cryst. Chem.* **1976**, *32*, 702–705.
- (19) Cailleau, H.; Girard, A.; Moussa, F.; Zeyen, C. M. E. Inelastic Neutron Scattering Study of Structural Phase Transitions in Polyphenyls. *Solid State Commun.* **1979**, *29*, 259–261.
- (20) Girard, A.; Cailleau, H.; Marqueton, Y.; Ecolivet, C. Raman Scattering Study of the Order-Disorder Phase Transition in *para*-Terphenyl. *Chem. Phys. Lett.* **1978**, *54*, 479–482.
- (21) Chang, S. S. Heat Capacity and Thermodynamic Properties of *p*-Terphenyl: Study of Order-Disorder Transition by Automated High-Resolution Adiabatic Calorimetry. *J. Chem. Phys.* **1983**, *79*, 6229–6236.
- (22) Friedman, P. S.; Kopelman, R.; Prasad, P. N. Spectroscopic Evidence for a Continuous Change in Molecular and Crystal Structure: Deformation of Biphenyl in the Low Temperature Solid. *Chem. Phys. Lett.* **1974**, *24*, 15–17.
- (23) Bree, A.; Edelson, M. A Study of the Second Order Phase Transition in Biphenyl at 40 K Through Raman Spectroscopy. *Chem. Phys. Lett.* **1977**, *46*, 500–504.
- (24) Atake, T.; Chihara, H. Heat Capacity Anomalies Due to Successive Phase Transitions in 1,1-Biphenyl. *Solid State Commun.* **1980**, *35*, 131–134.
- (25) Mazziotti, M. V.; Valletta, A.; Campi, G.; Innocenti, D.; Perali, A.; Bianconi, A. Possible Fano Resonance for High- T_c Multi-Gap Superconductivity in *p*-Terphenyl Doped by K at the Lifshitz Transition. *Europhys. Lett.* **2017**, *118*, 37003.
- (26) Furumoto, H. W.; Cecon, H. L. Ultraviolet Organic Liquid Lasers. *IEEE J. Quantum Electron.* **1970**, *6*, 262–268.
- (27) Saito, K.; Atake, T.; Chihara, H. Thermodynamic Studies on Order-Disorder Phase Transitions of *p*-Terphenyl and *p*-Terphenyl- d_{14} . *Bull. Chem. Soc. Jpn.* **1988**, *61*, 2327–2336.
- (28) Bolton, B. A.; Prasad, P. N. Phase Transitions in Polyphenyls: Raman Spectra of *p*-Terphenyl and *p*-Quaterphenyl in the Solid State. *Chem. Phys.* **1978**, *35*, 331–344.
- (29) Baudour, J. L.; Delugeard, Y.; Cailleau, H. Transition Structurale Dans Les Polyphényles. I. Structure Cristalline de la Phase Basse Température du *p*-Terphényle à 113 K. *Acta Crystallogr., Sect. B: Struct. Crystallogr. Cryst. Chem.* **1976**, *32*, 150–154.
- (30) Barba, L.; Chita, G.; Campi, G.; Suber, L.; Bauer, E. M.; Marcelli, A.; Bianconi, A. Anisotropic Thermal Expansion of *p*-Terphenyl: A Self-Assembled Supramolecular Array of Poly-*p*-Phenyl Nanoribbons. *J. Supercond. Novel Magn.* **2018**, *31*, 703–710.
- (31) Kohda, K.; Nakamura, N.; Chihara, H. Proton Magnetic Relaxation Study of Phase Transition in Crystalline *p*-Terphenyl. *J. Phys. Soc. Jpn.* **1982**, *51*, 3936–3941.
- (32) Bordat, P.; Brown, R. A Molecular Model of *p*-Terphenyl and Its Disorder-Order Transition. *Chem. Phys.* **1999**, *246*, 323–334.
- (33) Girard, A.; Sanquer, M.; Dëlugeard, Y. Low-Frequency Raman Study of *para*-Terphenyl: Influence of the Isotopic Substitution and Interpretation of the Spectra in Both Phases. *Chem. Phys.* **1985**, *96*, 427–434.
- (34) Girard, A.; Delugeard, Y.; Cailleau, H. Study of the Influence of Pressure on the *p*-Terphenyl Phase Transition by Raman Scattering. *J. Phys. (Paris)* **1987**, *48*, 1751–1759.
- (35) Toudic, B.; Launois, P.; Moussa, F.; Girard, A.; Cailleau, H. Pressure Dependence of Conformational Instabilities in Crystalline *p*-Terphenyl. *Ferroelectrics* **1988**, *80*, 241–244.
- (36) Murugan, N. A.; Yashonath, S. Pressure Induced Orientational Ordering in *p*-Terphenyl. *J. Phys. Chem. B* **2005**, *109*, 1433–1440.
- (37) Schatschneider, B.; Chronister, E. L. Molecular Simulation of the Pressure-Induced Crystallographic Phase Transition of *p*-Terphenyl. *J. Phys. Chem. B* **2011**, *115*, 407–413.
- (38) Liu, T.; Xu, S.; Sun, C.; Zhou, M. Raman Spectroscopic Studies on *p*-Terphenyl Under High Pressure. *Chem. Phys. Lett.* **2014**, *615*, 1–5.
- (39) Honda, K.; Furukawa, Y. Conformational Analysis of *p*-Terphenyl by Vibrational Spectroscopy and Density Functional Theory Calculations. *J. Mol. Struct.* **2005**, *735*, 11–19.
- (40) Zhang, K.; Chen, X. J. Chain Length Effects of *p*-Oligophenyls With Comparison of Benzene by Raman Scattering. *AIP Adv.* **2018**, *8*, 025004.
- (41) Heimel, G.; Somitsch, D.; Knoll, P.; Brédas, J.-L.; Zojer, E. Effective Conjugation and Raman Intensities in Oligo(*para*-

Phenylene)s: A Microscopic View From First-Principles Calculations. *J. Chem. Phys.* **2005**, *122*, 114511.

(42) Ohtsuka, H.; Furukawa, Y.; Tasumi, M. Dependencies of the Raman Spectra of *p*-Oligophenyls on the Chain Length and the Excitation Wavelength. *Spectrochim. Acta* **1993**, *49*, 731–737.

(43) Heibel, G.; Somitsch, D.; Knoll, P.; Zojer, E. Albrecht Theory and Anharmonic Coupling in Polyphenyl Raman Spectra. *Synth. Met.* **2003**, *139*, 823–825.

(44) Cuff, L.; Kertesz, M. *Ab initio* Oligomer Approach to Vibrational Spectra of Polymers: Comparison of Helical and Planar Poly(*p*-Phenylene). *Macromolecules* **1994**, *27*, 762–770.

(45) Heibel, G.; Somitsch, D.; Knoll, P.; Zojer, E. *Ab initio* Study of Vibrational Anharmonic Coupling Effects in Oligo(*para*-Phenylenes). *J. Chem. Phys.* **2002**, *116*, 10921–10931.

(46) Wilson, E. B., Jr. The Normal Modes and Frequencies of Vibration of the Regular Plane Hexagon Model of the Benzene Molecule. *Phys. Rev.* **1934**, *45*, 706–714.

(47) Angus, W. R.; Bailey, C. R.; Hale, J. B.; Ingold, C. K.; Leckie, A. H.; Raisin, C. G.; Thompson, J. W.; Wilson, C. L. Structure of Benzene. Part VIII. Assignment of Vibration Frequencies of Benzene and Hexadeuterobenzene. *J. Chem. Soc.* **1936**, *218*, 971–987.

(48) Ito, M.; Shigeoka, T. Raman Spectra of Benzene and Benzene- d_6 Crystals. *Spectrochim. Acta* **1966**, *22*, 1029–1044.

(49) Martin, C. M.; Cai, Q.; Guha, S.; Graupner, W.; Chandrasekhar, M.; Chandrasekhar, H. R. Raman Modes in Oligophenyls Under Hydrostatic Pressure. *Phys. Status Solidi B* **2004**, *241*, 3339–3344.